H^0+N_2 collisions at low-kilo-electron-volt energies

E. J. Quintana and E. Pollack
Department of Physics, University of Connecticut, Storrs, Connecticut 06269-3046
(Received 30 May 1995)

Direct scattering ($\rightarrow H^0$), stripping ($\rightarrow H^+$), and electron capture ($\rightarrow H^-$) are studied at energies of 1.0, 2.0, and 3.0 keV in small-angle H^0+N_2 collisions. Time-of-flight and electrostatic-energy analysis are used to identify the dominant collision processes. The electronically elastic channel is found to be weak beyond the very smallest scattering angles. As an example, at 1.0 keV, electronically inelastic processes dominate the collision for scattering angles larger than 0.2°. Beyond the smallest angles, both the stripping and electron-capture processes can also result in electronic excitation of the N_2 or N_2^+. The reduced cross sections, when plotted as a function of reduced scattering angle, are shown to scale reasonably well for each of the three processes studied.

PACS number(s): 34.50.Gb, 34.90.+q

I. INTRODUCTION

Collision studies generally provide information on the interactions that occur between a given projectile and target. Experimental results can test and in many cases guide the development of underlying theories. In this context there is a substantial literature on keV energy collisions that is dominated by studies of ion-atom problems. There are significantly fewer studies on ion-molecule collisions and only very limited work on atom-molecule systems. In this paper we report on H^0+N_2 at low-keV energies. In addition to the intrinsic interest in problems involving H^0, these collisions are particularly important at auroral altitudes. They affect the energy balances and the chemistry and must be understood for modeling calculations. The low-keV energy H^0, at auroral altitudes, has its origin in a much higher-energy H^+ flux (from the solar wind and other sources), which is incident on the upper atmosphere. The incident H^+ ions undergo inelastic collisions, resulting in the excitation and ionization of the target atoms and molecules. The projectiles are primarily scattered through small angles in each of these collisions and degrade to energies where electron-capture processes become important. Electron-capture collisions then generate H^0 and H^-, resulting in a mixed flux of the three charge states of hydrogen. At auroral altitudes the H^0 component has a low-keV energy distribution and is the dominant charge state. H^0 atoms at energies less than 10 keV cause most of the observed ionization and optical emissions from the auroral regions [1]. In addition, the H^0 atoms generate free electrons following stripping collisions. The collisional excitation of keV energy H^0 is also the major source of Lyman α in the hydrogen aurora. The radiation results from the excitation of $H(2p)$ in direct scattering rather than from electron capture in H^+ collisions [1]. It is clear that modeling calculations for upper atmospheric processes require some understanding of keV energy collisions such as H^0+N_2.

Although keV energy ion-molecule and atom-molecule collisions have been studied for a number of years, our understanding of them remains limited. Except for a few cases, a qualitative approach is often used to interpret experimental results. The approaches (see Refs. [2,3] as examples) are basically similar to those used successfully for atomic targets. On the basis of a state diagram, electronic excitation may occur via a ''Demkov'' process [4] between initial and final states for which the potential-energy curves are parallel. Electronic excitation may also occur at molecular orbital or state crossings. In He^+ collisions with CO and NO [3] it was shown that, as in the case of atomic targets, a correlated two-electron-transfer process leads to excitation and charge exchange. Electronically inelastic processes are generally found to be weak at low-keV energies for $\tau=E\theta$ (reduced scattering angle)=(beam energy)×(scattering angle) values smaller than 1 keV deg (see Refs. [3,5] as examples).

Relatively little work has been reported on H^0+N_2. As examples of the limited literature we cite the experimental charge production cross sections and differential scattering calculations of Van Zyl *et al.* [6], the electron-capture and -loss studies of Smith *et al.* [7], the differential and total scattering cross sections for stripping reported by Cisneros *et al.* [8], and the absolute differential cross sections for very-small-angle scattering reported by Johnson *et al.* [9]. In this paper we present results of a study of the direct scattering [$H^0(1s)+N_2\rightarrow H^0$, including the elastic and electronically inelastic channels], as well as of the stripping [$H^0(1s)+N_2\rightarrow H^+$], and electron-capture [$H^0(1s)+N_2\rightarrow H^-$] processes. The present work, using time-of-flight techniques for energy-loss measurements on H^0 and electrostatic energy analysis on H^+ and H^-, presents results on the angular dependence of the collision processes at energies of 1.0, 2.0, and 3.0 keV. It is shown that inelastic collisions are dominant beyond the smallest angles in $H^0(1s)+N_2$ and that excitation of the final N_2 or N_2^+ must be considered in accurate calculations on the stripping or electron capture.

II. EXPERIMENTAL TECHNIQUES

The experimental techniques have been previously described [10,11] and are only outlined here. Figure 1 shows the experimental arrangement. H^+ is extracted from a Colutron ion source floated at a low-kV voltage, which determines the beam energy. The source is supplied with a mixture of H_2 and Ar to increase the long-term stability of the beam when compared to using pure H_2. The beam is focused by an einzel lens, passed through a set of shim fields into a

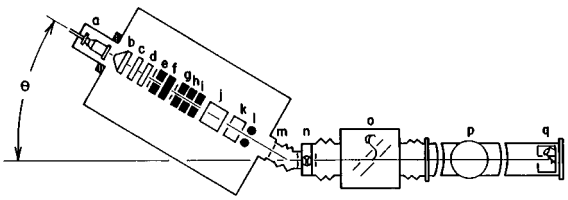

FIG. 1. Schematic of the experimental arrangement: ion source (a), extractor and einzel lenses ($b-d$), deflectors ($e-i$), Wien filter (j), charge-exchange cell (k), deflector plates (l), scattering cell (m), valve (n), electrostatic energy analyzer (o), cryopump (p), and time-of-flight (TOF) detector (q). The distance from the scattering cell to the TOF detector is 4.2 m.

beam ''chopping region'' consisting of two plates (about 1 cm long and separated by 0.5 cm), and is chopped by a voltage pulsed at 0.3 MHz for the time-of-flight measurements. It is mass analyzed by a Wien filter and then passes through a charge exchange cell filled with H_2. A composite H^+ and H^0 beam emerges from the charge exchange cell. The H^+ is electrically deflected leaving an H^0 beam, which enters the scattering cell containing the N_2 target gas at pressures within the single collision region. The projectiles scatter through an angle θ and enter an electrostatic analyzer for energy measurements on H^+ and H^-. The H^0 passes through the analyzer to a time-of-flight detector positioned 4.2 m from the scattering cell. The initial H^+ beam (prior to neutralization) has an energy full width at half maximum (FWHM) of 0.5 eV per keV and a FWHM angular spread of 0.1°. Following electron capture, the H^0 has a measured FWHM energy spread of 2.0 eV at 1.0 keV and a FWHM angular spread of 0.15°.

Energy-loss spectra are acquired at selected angles in the direct scattering ($H^0+N_2\rightarrow H^0$). Since the direct scattering does not involve a change in charge state, the incident H^0 beam provides the energy reference from which the states are identified. The probability of elastic scattering at each angle is determined from the ratio of the number of counts in the elastic peak to the total number of counts in the H^0 spectrum. The probabilities for the inelastic channels are determined the same way. A ''summed cross section'' is obtained from a measurement of the angular distribution of the scattered H^0 without energy analysis. Summed cross sections at $E=0.5$, 1.5, and 5.0 keV were also reported by Johnson *et al.* [9]. Their summed results show a slight undulation (near 0.2° at 1.5 keV as an example). Because of the significant loss in beam intensity (due to chopping) in time-of-flight measurements, the angular resolution in the present studies cannot be as high as in Ref. [9] and this weak structure is not seen. The elastic cross section at each energy is found by multiplying the summed cross section by the probability of elastic scattering. The stripping channels are studied in a similar manner. Here spectra are acquired for the H^+ and the summed cross sections for stripping are obtained from the angular distributions of the scattered H^+ (without energy analysis). Similar techniques are used for studying electron capture. Since there are changes in charge state for stripping and capture collisions, energy references are needed and obtained from $H^0(1s)+Ar\rightarrow H^+/H^-$ collisions.

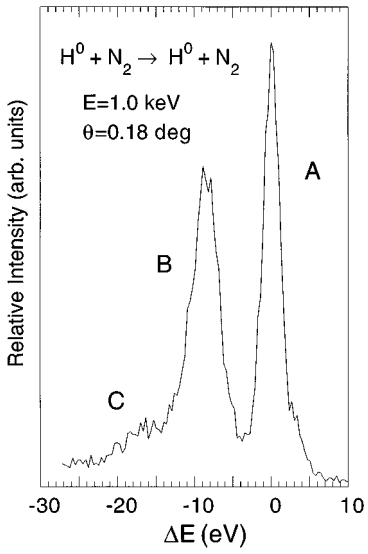

FIG. 2. Typical energy-loss spectrum for the direct scattering in H^0+N_2 at an energy $E=1.0$ keV and scattering angle $\theta=0.18°$. The electronically elastic peak is labeled A. Peaks B and C result from inelastic processes.

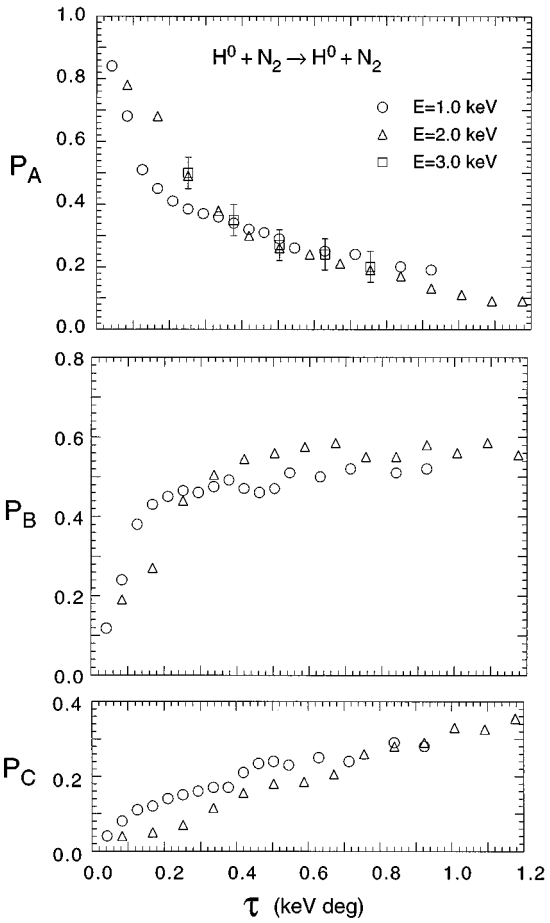

FIG. 3. Probabilities for electronically elastic scattering (P_A) and for the excitation of electronically inelastic processes (P_B and P_C) plotted as a function of reduced scattering angle $\tau=E\theta$. The electronically inelastic processes are seen to dominate beyond reduced scattering angles of 0.2 keV deg.

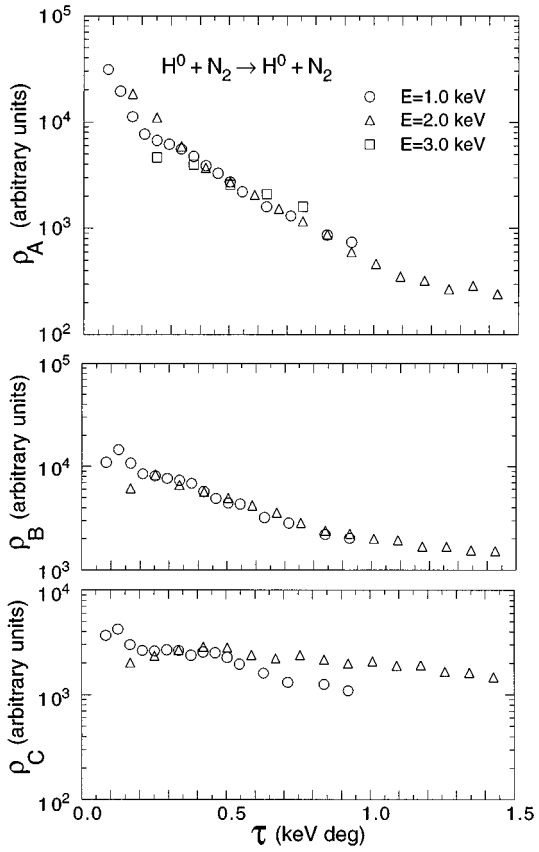

FIG. 4. Reduced differential cross sections as a function of reduced scattering angle for the processes corresponding to peaks $A-C$ in Fig. 1. The results are plotted to different arbitrary units and show that they can be approximated by common curves.

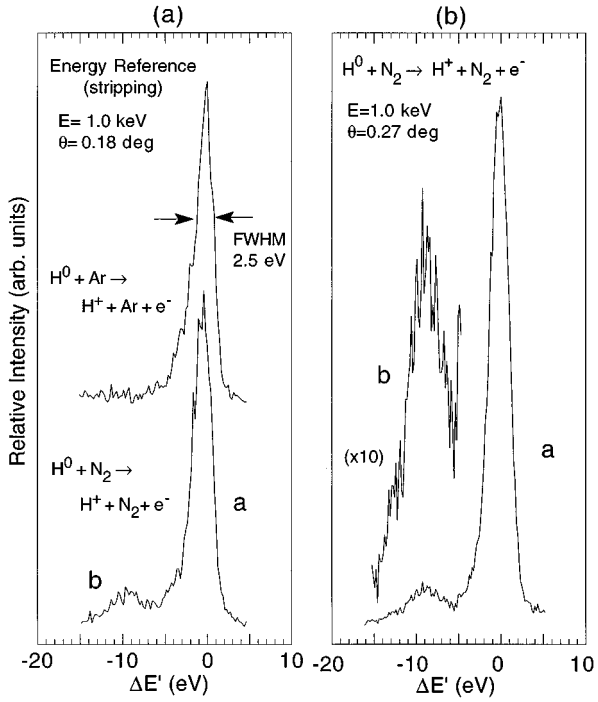

FIG. 5. (a) Composite spectra from $H^0+N_2 \rightarrow H^+$ and $H^0+Ar \rightarrow H^+$. $\Delta E'$ $(=\Delta E-13.6$ eV) is set to zero at the maximum of peak a. Using the Ar results, the dominant process in N_2 is seen to be $H^0(1s)+N_2(X) \rightarrow H^+ + N_2(X) + e^-$. (b) Typical energy-loss spectrum for stripping in H^0+N_2. Two peaks are seen and attributed to (a) $H^+ + N_2(X)$ and (b) $H^+ + N_2{}^*$.

III. EXPERIMENTAL RESULTS AND CONCLUSIONS

We are studying the small-angle direct scattering, stripping, and electron capture for $H^0(1s)+N_2$ collisions at energies of 1.0, 2.0, and 3.0 keV. The underlying collision processes are identified using Gilmore's potential-energy curves for N_2 [12] and assuming that electronic excitations occur via Franck-Condon transitions from the $N_2(X\ ^1\Sigma_g^+,\ \nu=0)$ level. Figure 2 shows a typical energy-loss spectrum for the direct scattering in H^0+N_2 ($E=1.0$ keV, $\theta=0.18°$). The peak labeled A corresponds to electronically elastic scattering. Peak B results from the excitation of a number of electronically inelastic processes. The maximum at an energy loss ΔE near 9 eV is consistent with the excitation of any in a group of N_2 states ($a\ ^1\Pi_g$, $a'\ ^1\Sigma_u^-$, $B'\ ^3\Sigma_u^-$, and $w\ ^1\Delta_u$). Contributions to the spectrum at an energy loss $\Delta E \approx 8$ eV may result from excitation of the $N_2(B\ ^3\Pi_g)$ state. It is unusual, however, that the $N_2(A\ ^3\Sigma_u^+)$ state is only weakly excited. The excitation of triplet states from an initial N_2 singlet state is not allowed in H^+ collisions but can occur when H^0 projectiles are used. At energy losses ΔE between 11 and 12 eV the peak's shape suggests possible contributions from both the N_2 $C\ ^3\Pi_u$ and $E\ ^3\Sigma_g^+$ states. The excitation of H^0 $(n=2)$ at $\Delta E=10.2$ eV is also within the range of peak B and cannot be discounted. The small structure (peak C) at $\Delta E>15$ eV, seen primarily at larger τ values, can be associated with ionization of the molecule and one electron excitation of the higher-lying Rydberg series of N_2. Peak C is also consistent with the simultaneous excitation of single electron states in both the H^0 and N_2. Figure 3 shows the probabilities for electronically elastic scattering (P_A) and for the inelastic processes (P_B and P_C) as a function of τ, the reduced scattering angle, at energies of 1.0, 2.0, and 3.0 keV. The electronically inelastic processes are seen to dominate the collision beyond τ values of 0.2 keV deg. Figure 4 shows ρ $[=\theta \sin\theta\sigma(\theta)]$, the reduced differential cross sections, plotted as a function of τ and normalized to show that the general behavior for these processes can be approximated by common curves at the energies studied.

Stripping of the electron from the H^0 projectile involves a minimum energy loss of 13.6 eV. Since there is a change in the projectile charge state, an energy reference is required for interpreting the H^+ spectra. The reference is obtained from $H^0(1s)+Ar \rightarrow H^+$ collisions. Figure 5(a) shows composite spectra for $H^0+Ar \rightarrow H^+$ and $H^0+N_2 \rightarrow H^+$. The main peaks for the Ar and N_2 targets have the same basic shape (FWHM of 2.5 eV) and the locations of the maxima show that the dominant stripping process in N_2 results in $H^+ + N_2(X) + e^-$. The FWHM is greater than the 0.5 eV associated with the incident beam at $E=1.0$ keV and is attributed in part to the kinetic energy carried off by the ejected electrons. Figure 5(b) shows an enlarged plot of a second process (labeled b) with energy losses (relative to peak a) in the range of 6.5–12 eV. The peak is attributed to stripping with simultaneous excitation of the N_2. Stripping resulting in H^0 $(1s)+N_2 \rightarrow H^+ + N_2^-$ ($\Delta E=1.6$ eV relative to stripping at threshold to the continuum) is found to be weak. Although the N_2^- state is unstable [12], its collisional excitation would be seen in

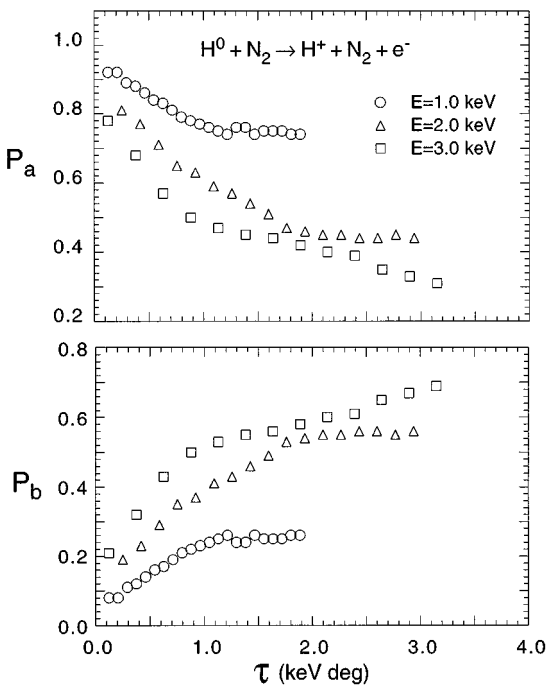

FIG. 6. Probabilities for stripping as a function of reduced scattering angle in H^0+N_2. P_a corresponds to $H^++N_2(X)$ and P_b to H^++N_2*, where the target is electronically excited.

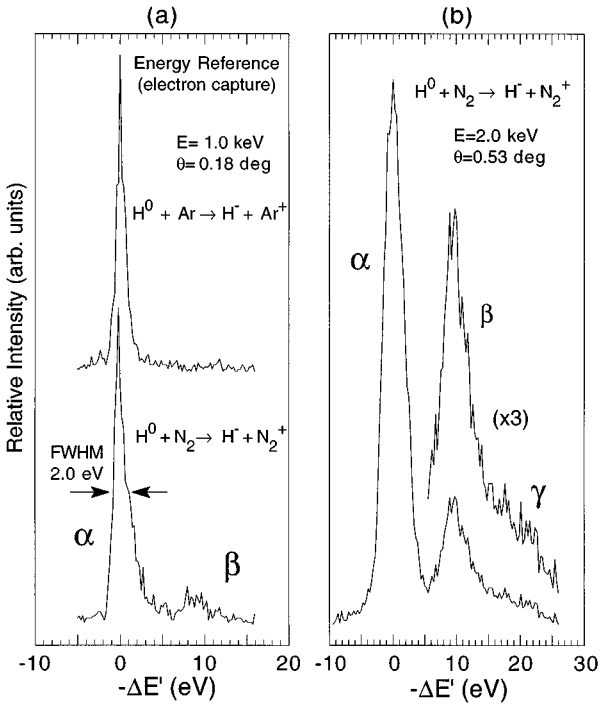

FIG. 8. (a) Energy reference for electron capture showing that the dominant process is $H^0+N_2 \rightarrow H^-+N_2^+$. $\Delta E'$ ($=\Delta E-15$ eV) is set to zero at the maximum of peak α. (b) Typical energy spectrum for electron capture in H^0+N_2. Two main peaks (α)$\rightarrow H^-(1s^2)+N_2^+(X)$ and (β)$\rightarrow H^-(1s^2)+N_2^+$* and a tail ($\gamma$) are seen. Possible contributions to peak β from H^-*$+N_2^+$ cannot be ruled out. The energy-loss scale is reversed here since the detected beam is negatively charged.

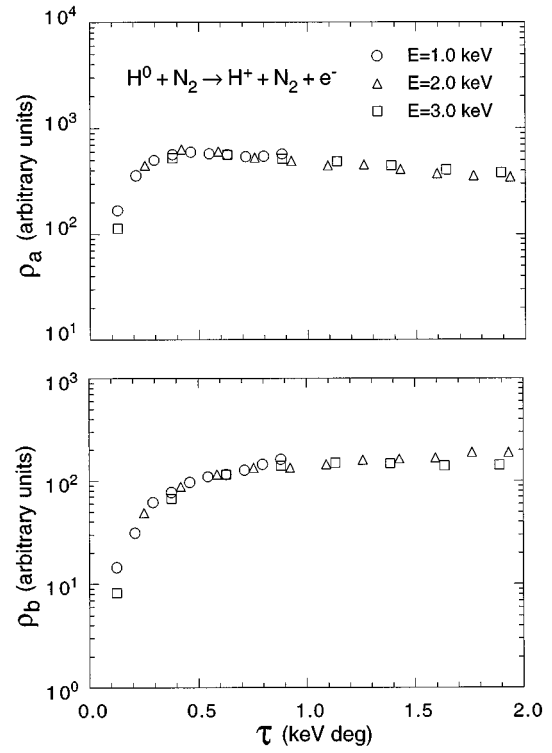

FIG. 7. Reduced cross sections as a function of reduced scattering angle for simple stripping (ρ_a) and stripping with target excitation (ρ_b) in H^0+N_2. The results are plotted to different arbitrary units and show that the shapes are well approximated by common curves at the three energies studied.

the H^+ spectra. Previous studies of charge-changing collisions have focused on absolute differential and total [6–8] cross-section measurements for the summed channels. Our results for the summed channels show the same qualitative features as reported in Ref. [7]. Figure 6 shows P_a and P_b, the probabilities of processes a and b plotted against τ. Figure 7 shows the reduced differential cross sections for stripping. The normalized results for ρ_a and ρ_b scale well for the three energies studied.

In the H^0+N_2 electron-capture processes an electron is transferred from the molecular target with an energy loss ΔE of at least 14.7 eV. An energy calibration at 1.0 keV using $H^0+Ar \rightarrow H^-+Ar^+$ and a typical spectrum from $H^0+N_2 \rightarrow H^-$ are shown in Fig. 8(a). The H^0+Ar calibration shows that the dominant process in N_2 (peak labeled α) corresponds to H^- $(1s^2)+N_2^+(X)$. The spectrum in Fig. 8(b) at $E=2.0$ keV and $\theta=0.52°$ shows a weaker process (β) with a maximum positioned 10 eV down in energy and a tail (γ). The peak (β) is consistent with electron capture to $H^-+N_2^+$ ($C\ ^2\Sigma_u^+$ and $D\ ^2\Pi_g$). The probabilities for electron capture to processes α, β, and γ are plotted as a function of reduced scattering angle in Fig. 9. The reduced differential cross sections for electron capture are shown in Fig. 10. These cross sections are again reasonably well fitted by common curves at the energies studied.

At low-keV energies atom-atom and the few atom-molecule systems studied (see Refs. [3,5] as examples) generally show strong elastic scattering at small scattering

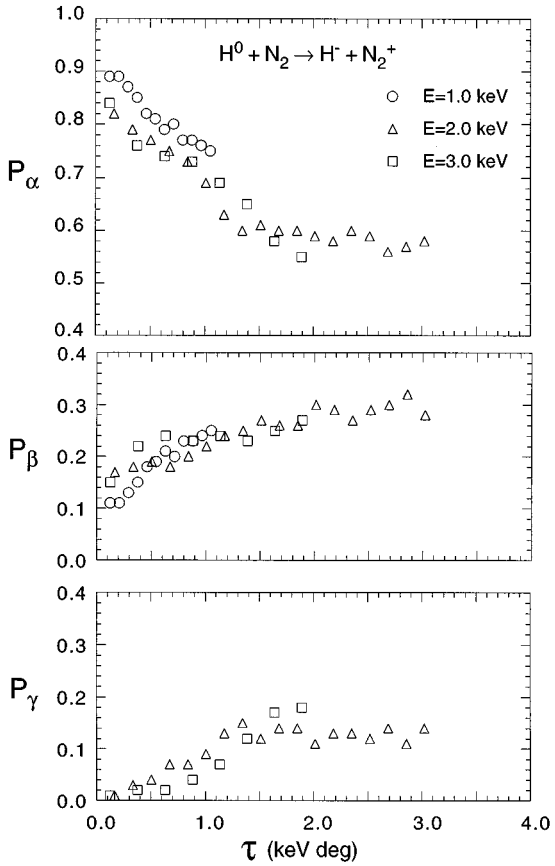

FIG. 9. Probabilities for electron capture as a function of reduced scattering angle in H^0+N_2. P_α results from capture to $H^-(1s^2)+N_2^+(X)$, P_β to $H^-(1s^2)+N_2^+*$, and P_γ to $H^-(1s^2)$ with the excitation of highly excited N_2^+ states.

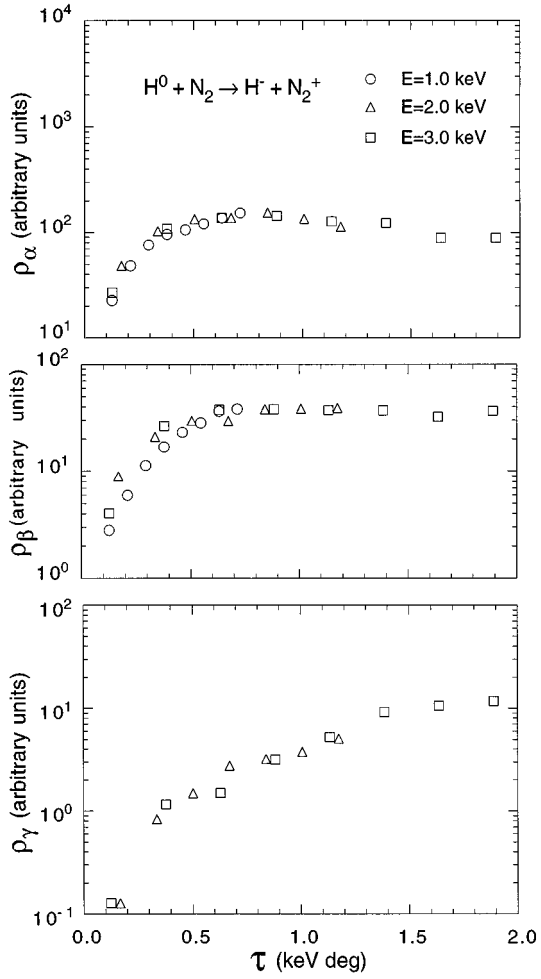

FIG. 10. Reduced differential cross sections for electron capture to (α) $H^-(1s^2)+N_2^+(X)$, (β) $H^-(1s^2)+N_2^+*$, and (γ) $H^-(1s^2)+N_2^+*$ as a function of reduced scattering angle in H^0+N_2. The results are plotted to different arbitrary units and are seen to be reasonably well fitted by common curves.

angles. Direct inelastic processes become important at larger angles. A significant result of this study is that in $H^0(1s)+N_2$ the inelastic processes are found to dominate the collision beyond the smallest angles (τ>0.2 keV deg). In a paper on charge production in H^0+N_2, Van Zyl *et al.* [6] suggested that ionic states play an important role in the collision. Our present results support the role of the ionic channel even in the direct scattering. The lowest-lying $H^-+N_2^+$ state is positioned, for infinite separation, at an energy of 15 eV above the incident $H+N_2$ potential-energy curve. Since the ionic channel is attractive, the repulsive incident channel must cross it. The crossing may result in the excitation of an intermediate ionic channel. Following the excitation of $H^-+N_2^+$, this state can couple via Demkov [4] or curve crossing processes to excited states resulting in H^*+N_2 or $H(1s)+N_2^*$. The importance of the electronically inelastic channels in small-angle $H(1s)+N_2$ collisions supports this model since an intermediate attractive channel would result in smaller scattering angles for the processes it excites. It is particularly interesting that the normalized reduced differential cross sections for all the direct channels (elastic and inelastic), the stripping, and electron-capture processes are reasonably well fitted by common curves when plotted as a function of the reduced scattering angle. A careful comparison of the reduced cross section for stripping with target excitation (ρ_b) to electron capture with target excitation (ρ_β) shows an almost identical behavior in the angular dependence of the two cross sections. This suggests that a common primary interaction excites the two channels.

ACKNOWLEDGMENTS

This work was supported by the Connecticut Space Grant College Consortium under NASA Grant No. NGT-40037 and the University of Connecticut Research Foundation. We wish to thank Dr. Valerie Heckman for her contributions to the research.

[1] R. J. McNeal and J. H. Birely, Rev. Geophys. Space Phys. **11**, 663 (1973).
[2] W. L. Hodge, Jr., A. L. Goldberger, M. Vedder, and E. Pollack, Phys. Rev. A **16**, 2360 (1977).
[3] D. Dowek, D. Dhuicq, and M. Barat, Phys. Rev. A **28**, 2838 (1983).
[4] Y. N. Demkov, Zh. Eksp. Teor. Fiz. **45**, 195 (1963) [Sov. Phys. JETP **18**, 138 (1964)].
[5] J. Jakacky, Jr., E. Pollack, R. Snyder, and A. Russek, Phys. Rev. A **31**, 2149 (1985).
[6] B. Van Zyl, H. Neumann, T. Q. Le, and R. C. Amme, Phys. Rev. **18**, 506 (1978).
[7] G. J. Smith, L. K. Johnson, R. S. Gao, K. A. Smith, and R. F. Stebbings, Phys. Rev. A **44**, 5647 (1991).
[8] C. Cisneros, I. Alvarez, C. F. Barnett, and J. A. Ray, Phys. Rev. A **14**, 84 (1976).
[9] L. K. Johnson, R. S. Gao, K. A. Smith, and R. F. Stebbings, Phys. Rev. A **38**, 2794 (1988).
[10] Q. C. Kessel, E. Pollack, and W. W. Smith, in *Collisional Spectroscopy*, edited by R. G. Cooks (Plenum, New York, 1977), Chap. 2.
[11] E. Pollack and Y. Hahn, Adv. At. Mol. Phys. **22**, 243 (1986).
[12] F. R. Gilmore, J. Quant. Spectrosc. Radiat. Transf. **5**, 369 (1965).